water

MDPI

Article

Comparison of Three Techniques to Adjust Daily Precipitation Biases from Regional Climate Models over Germany

Chibuike Chiedozie Ibebuchi [1,*], Daniel Schönbein [1], Muralidhar Adakudlu [2], Elena Xoplaki [2,3] and Heiko Paeth [1]

[1] Institute of Geography and Geology, University of Würzburg, Am Hubland, 97074 Würzburg, Germany; daniel.schoenbein@uni-wuerzburg.de (D.S.); heiko.paeth@uni-wuerzburg.de (H.P.)
[2] Center for International Development and Environmental Research, Justus Liebig University Giessen, 35390 Giessen, Germany; muralidhar.adakudlu@zeu.uni-giessen.de (M.A.); elena.xoplaki@geogr.uni-giessen.de (E.X.)
[3] Department of Geography, Justus Liebig University Giessen, 35390 Giessen, Germany
* Correspondence: chibuike.ibebuchi@uni-wuerzburg.de

Abstract: This study compares the performance of three bias correction (BC) techniques in adjusting simulated precipitation estimates over Germany. The BC techniques are the multivariate quantile delta mapping (MQDM) where the grids are used as variables to incorporate the spatial dependency structure of precipitation in the bias correction; empirical quantile mapping (EQM) and, the linear scaling (LS) approach. Several metrics that include first to fourth moments and extremes characterized by the frequency of heavy wet days and return periods during boreal summer were applied to score the performance of the BC techniques. Our results indicate a strong dependency of the relative performances of the BC techniques on the choice of the regional climate model (RCM), the region, the season, and the metrics of interest. Hence, each BC technique has relative strengths and weaknesses. The LS approach performs well in adjusting the first moment but tends to fall short for higher moments and extreme precipitation during boreal summer. Depending on the season, the region and the RCM considered, there is a trade-off between the relative performances of the EQM and the MQDM in adjusting the simulated precipitation biases. However, the MQDM performs well across all considered metrics. Overall, the MQDM outperforms the EQM in improving the higher moments and in capturing the observed return level of extreme summer precipitation, averaged over Germany.

Keywords: bias correction; multivariate quantile delta mapping; empirical quantile mapping; linear scaling; precipitation; Germany

Citation: Ibebuchi, C.C.; Schönbein, D.; Adakudlu, M.; Xoplaki, E.; Paeth, H. Comparison of Three Techniques to Adjust Daily Precipitation Biases from Regional Climate Models over Germany. *Water* **2022**, *14*, 600. https://doi.org/10.3390/w14040600

Academic Editor: Aizhong Ye

Received: 12 January 2022
Accepted: 14 February 2022
Published: 16 February 2022

1. Introduction

Despite the higher horizontal resolution of regional climate models (RCMs) compared to general circulation models (GCMs), simulated precipitation from RCMs exhibits systematic biases relative to observations [1]. Since RCMs are tools used to project future climate change at a regional scale [2,3], the systematic biases can result in unrealistic interpretations of future climate change signals (e.g., [4]). Thus, there is the need for bias correction (BC) of the RCMs before their usage in impact modeling and adaptation studies.

Bias correction can be considered as a part of the model evaluation. For post-processing a climate model, BC uses the relationship between the observed variable and climate model simulations [5]. Given that the temporal variations between climate simulations and observations are not in the same phase, e.g., due to initial boundary conditions that are largely determined by the driving GCM, statistical post-processing with BC is usually focused on improving the distributional aspects (e.g., moments and quantiles) of the simulated variable to be closer to the corresponding observed variable. The systematic biases in model outputs can result from large-scale circulation biases from the GCM that provides the lateral boundary conditions, for example, a misrepresentation of the frequency

of weather types and position of the storm tracks, the parameterization of convection, unresolved sub-grid scale orographic effects, limited model complexity, and uncertain internal variability (e.g., [6]). Most state-of-the-art BC approaches do not improve the circulation biases and the biases associated with the uncertainties in internal variability but can be expected to adjust the biases associated with parameterizations and model resolution [7].

Several techniques have been developed to overcome some limitations faced by BC of climate models when used for climate change impact studies [8], e.g., cross-validated multiple regression models for mean value statistics [9,10]. Studies have also addressed BC techniques that improve extreme value statistics, using process-based and stochastic weather generators (e.g., [11]). Specifically, the empirical quantile mapping approach (EQM) that matches the quantiles of the simulated variable to a reference observed distribution, has been reported to outperform BC techniques in hydrological studies that focus on other distributional properties such as mean, median, or variance [12]. Nonetheless, the performance of BC techniques can be dependent also on the region and variable analyzed (e.g., [13]). Moreover, the EQM still faces several limitations, such as misrepresentation of variance of the corrected variable when the projected changes are not within the range of the historical distribution used as a reference for the bias correction [14]. Consequently, this can modify the projected trends—mostly trends in extreme quantiles (e.g., [15]). Hence, improved versions of EQM have been developed, such as parametric quantile mapping [16] that replaces the empirical distribution with appropriate parametric distribution, and detrended quantile mapping [17] that incorporates projected changes in the mean of the bias-corrected variable. Anyway, the parametric quantile mapping still follows the stationarity assumption (i.e., the transfer function obtained in the historical simulations is applicable under future climate change), which is questionable given the complexity and nonlinearity of future climate change. The detrended quantile mapping preserves the climate change signal only in the mean, ignoring other aspects of the distribution. To this end, the quantile delta mapping (QDM) [14] represents an efficient alternative to the univariate EQM since it corrects both the systematic biases and also preserves the projected future changes in the quantiles. Hence with QDM, the assumption of a stationary transfer function is no longer necessary.

Within the regional context of Germany, the relative performances of a wide range of BC techniques have been implemented. For example, over the Bavarian catchments, ref. [18] evaluated the relative performances of linear scaling (LS) [19], local intensity scaling, and quantile mapping in improving RCMs for runoff modeling. They found that while the mean flow is well represented, the extreme flow is poorly reproduced by all the considered methods; the quantile mapping, however, outperforms the scaling approach. A similar result was reported by [20], where the performance of simpler methods was limited to improving the simulated mean values.

Furthermore, univariate BC methods do not consider inter-variable dependency. According to [21], the application of univariate quantile mapping at each grid point in the study region can alter the spatial variability of the simulated variable, which might modify the underlying spatial atmospheric modes and physics. In this respect, studies have examined the added value of multivariate BC techniques. Commonly, a copula theory—i.e., the consideration of the joint dependency of variables in the course of the BC [22]—is used in multivariate bias corrections. Over Germany, ref. [23] found that a stochastic BC technique, based on the concept of copula theory, performs better than quantile mapping in adjusting precipitation biases. Similarly, incorporating zero precipitation values, ref. [24] found that the copula-based scheme performs well in Germany both for mean and extreme conditions. Moreover, the implementation of multivariate bias corrections commonly relies on univariate bias correction algorithms to match the simulated multivariate distribution to the observed multivariate distribution [14]. On this ground, ref. [25] introduced a multivariate aspect of the QDM (MQDM). The MQDM is designed to transfer the entire multivariate distribution and the empirical copula. Using the MQDM, ref. [25] included

neighboring grid points as additional variables to incorporate the spatial dependency structure of precipitation in the BC. Here we applied the obliquely rotated S-mode (i.e., the variable is grid points and observation is time series) principal component analysis to regionalize precipitation in Germany. Hence in this study, sub-grid points in Germany that covary over time, with respect to precipitation, are used as the additional variables. Relative improvements in using the MQDM to correct daily precipitation estimates from two RCMs over Germany are compared to standard LS and EQM approaches. We score the performances based on the first to the fourth moments of precipitation distributions and extreme precipitation characterized by return period analysis.

Data and methods, in particular the compared BC techniques, are described in the next section. Section 3 is dedicated to the results and discussion, and conclusions are drawn in Section 4.

2. Data and Methods

2.1. Data

Simulated precipitation data is obtained from two CMIP5 EURO-CORDEX RCMs [26]. The RCMs are CCLM4 and REMO2015, each driven by the ERA-Interim and the MPI-ESM-LR GCM [27]. The ERA-Interim driven RCMs are used to evaluate the RCMs against gridded observed precipitation data from E-OBS [28]. The selection of the evaluation period 1989–2008 corresponds to the availability of all datasets. The RCMs driven by the GCM output under the historical experiment are obtained from 1950 to 2005 because they overlap with the E-OBS data. The temporal resolution of all data sets is daily. The spatial resolution of the RCMs is 0.11°, and 0.1° for E-OBS. The RCMs are further interpolated to the 0.1° longitude and latitude of the E-OBS data using first-order conservative remapping [29].

2.2. Bias Correction Techniques

We compared the performance of three BC techniques in adjusting the systematic biases in the precipitation field over Germany. The BC techniques are LS, EQM, and MQDM. The techniques are applied to the daily precipitation simulated output of the two RCMs driven by MPI-ESM-LR and ERA-Interim. The BC transfer functions are obtained at a seasonal time scale (i.e., conditioning the daily precipitation estimates by seasons) for the four seasons in the study region—i.e., winter (DJF), spring (MAM), summer (JJA), and autumn (SON). For the two univariate methods (i.e., LS and EQM), the transfer functions are obtained and applied at each grid point in Germany. For MQDM, the spatial heterogeneity of the precipitation field was simplified by using rotated S-mode principal component analysis (PCA) to obtain grid points that covary over time. The leading modes of the PCA, which reduce the spatial complexity of the precipitation field while retaining most of its variability, aid in obtaining optimized patterns, which are treated as additional variables (see Figure A1). Hence, the MQDM is applied to the sub-grids to improve the spatial dependency structure of the precipitation field in the course of the BC. The rationale behind using PCA to reduce the spatial complexity of the field is that the consideration of all grid points over Germany as covariates (rather than sub-grids that covary), implies an immense dimensionality of the spatiotemporal field and, hence, might lead to overfitting in the statistical models.

The analysis period, i.e., 1950–2005, is divided into two halves—1950 to 1977 and 1978 to 2005. The first half is the training period for which the BC transfer function is estimated, and the second half is the validation period. The transfer function is assumed to be stationary for the LS and EQM methods; but since the MQDM is implemented using QDM, climate change signals are incorporated in the course of the BC. As a result, the stationarity assumption is not necessary under the MQDM technique.

2.2.1. Linear Scaling

The LS approach is among the simplest BC techniques. It adjusts the biases in the mean based on Equation (1).

$$\hat{x}_{m,f}(t) = x_{m,f}(t) \times \left(\frac{\overline{x}_{o,h}}{\overline{x}_{m,h}} \right) \quad (1)$$

with

$x_{m,f}(t)$ = Raw modeled precipitation estimate, in mm/day, at time t in the validation period;
$\hat{x}_{m,f}(t)$ = Corrected modeled precipitation estimate, in mm/day, at time t in the validation period;
$\overline{x}_{o,h}$ = Seasonal mean of the observed precipitation estimate, in mm/day, during the training period;
$\overline{x}_{m,h}$ = Seasonal mean of the modeled precipitation estimate, in mm/day, during the training period.

2.2.2. Empirical Quantile Mapping

In the EQM, the transfer function is based on the cumulative distribution function (CDF). The transfer function is obtained by matching the quantiles of simulated daily precipitation estimates to that of the observed precipitation estimates during the validation period, according to Equation (2).

$$\hat{x}_{m,f}(t) = F_{o,h}^{-1}\left\{ F_{m,h}\left[x_{m,f}(t) \right] \right\} \quad (2)$$

$F_{o,h}$ = Observed CDF from the observational data in the training period;
$F_{m,h}$ = Modeled CDF from the simulated data in the training period.

The major limitation of the EQM is the stationarity assumption of the CDF. Since the algorithm relies on the historical CDF to correct future projections (Equation (2)), problems can be encountered when the forecast data is outside the range of the historical values, which is plausible when there is a strong climate change signal. As a consequence, projected trends can be affected in an undesirable way.

2.2.3. Quantile Delta Mapping

The QDM is an improved version of the EQM. Instead of the stationarity assumption in the EQM, the QDM is designed to preserve the model's relative changes in the quantiles [14]. As outlined in [14], there are two steps followed by the QDM to preserve the projected changes in the simulated quantiles: (i) before the quantile mapping, model outputs are detrended by quantile so that simulated historical and projected values take the characteristics of the historical observations without considering the change signal; (ii) projected relative changes in the simulated quantiles are super-imposed on the corrected values. The aim of step (ii) is to incorporate the climate change signal. These steps are described further in Equations (3)–(5), as implemented in [14] from where the equations were adapted.

$$\Delta(t) = \frac{x_{m,f}(t)}{F_{m,h}^{-1}\left[\tau_{m,f}(t) \right]} \quad (3)$$

with

$\tau_{m,f}(t)$ = The non-exceedance probability (ranging from 0 to 1) of the projected value at a given time in the validation/forecast period;
$F_{m,h}^{-1}$ = Inverse CDF of the simulated value during the historical/training period for the original values;
$\Delta(t)$ = Relative change signal in the simulated quantiles.

For a zero-bounded and right-skewed variable such as precipitation, $\Delta(t)$ is the ratio of the raw projected model output (i.e., in the forecast period or validation period), to the

model output in the historical period or training period. The bias-corrected quantile is given by

$$\hat{x}_{o:m,\ h:p}(t) = F_{o,h}^{-1}\left\{\tau_{m,f}(t)\right\} \quad (4)$$

with $\hat{x}_{o:m,\ h:p}(t)$ being the corrected quantile in the forecast period using the inverse CDF of observed values over the historical simulations. The final bias-corrected quantiles with climate change signal are obtained by

$$\hat{x}_{m,p}(t) = \hat{x}_{o:m,\ h:p}(t)\Delta(t) \quad (5)$$

2.2.4. Multivariate Quantile Mapping

The MQDM is the multivariate version of the QDM. A detailed explanation of the algorithm is given by [25] and the equations were adapted from the study. It transfers the full multivariate distribution and the empirical copula. Here we outline the basic steps:

(1) Apply orthogonal rotation to the 3 precipitation data sets respectively (i.e., the observed and simulated data in the training period, and the simulated precipitation data in the validation period). The rotation aims to (i) obtain a linear combination of the covariates and; (ii) obtain a uniform multivariate distribution that allows convergence between the simulated and observed multivariate distributions. Here the variables that are rotated to obtain the uniform multivariate distribution are grid points that covary over time.
(2) Match the simulated multivariate distribution (i.e., from the RCM) to fit the target multivariate distribution (i.e., from the observed precipitation) using QDM.
(3) Apply inverse rotation to the matched multivariate distribution in step (2).

Iteratively repeat steps (1) to (3) until the multivariate distribution of the simulated data converges to the multivariate distribution of the observed data.

2.3. Metrics Used to Validate the Bias Correction Techniques

The validation of the performance of the BC is done over the 1978–2005 period. For the seasonal time series of the corrected model outputs averaged over Germany, we calculated the first to fourth moments of the bias-corrected precipitation distribution and compared them with the observed values. The mean absolute error (MAE) was used to evaluate the performance of the corrected daily values at each grid point, both for spatial means and spatial variability (i.e., the standard deviation) of precipitation.

To assess the performance of the BC techniques with respect to extreme values, which is of major importance in modeling hydrological extremes, we calculate return times. First, during JJA when most parts of Germany receive their highest rainfall amounts and are prone to floods, the annual maxima of the precipitation data series averaged over Germany are obtained. Using the maximum likelihood estimation method, the generalized extreme value (GEV) distribution is fitted to the annual maximum precipitation series. Return time between 2 and 150 years is calculated and the simulated results from the bias-corrected output are compared to observed values using MAE. To ensure the robustness of the results from the annual maxima and GEV distribution, the return time calculations are repeated using a peak over threshold approach based on the Gumbel distribution.

3. Results and Discussion

3.1. Evaluation of Simulated Precipitation from Uncorrected RCMs

Figure 1a shows the mean annual cycle of precipitation, averaged over Germany, from the RCMs and E-OBS. The RCMs mainly capture the observed annual cycle. However, it can be seen that when ERA-Interim is used as driving data for the RCMs, the monthly precipitation sums are closer to the observed ones. The GCM-RCM model chain induces a wet bias at most of the grid points, especially in the CCLM4 model.

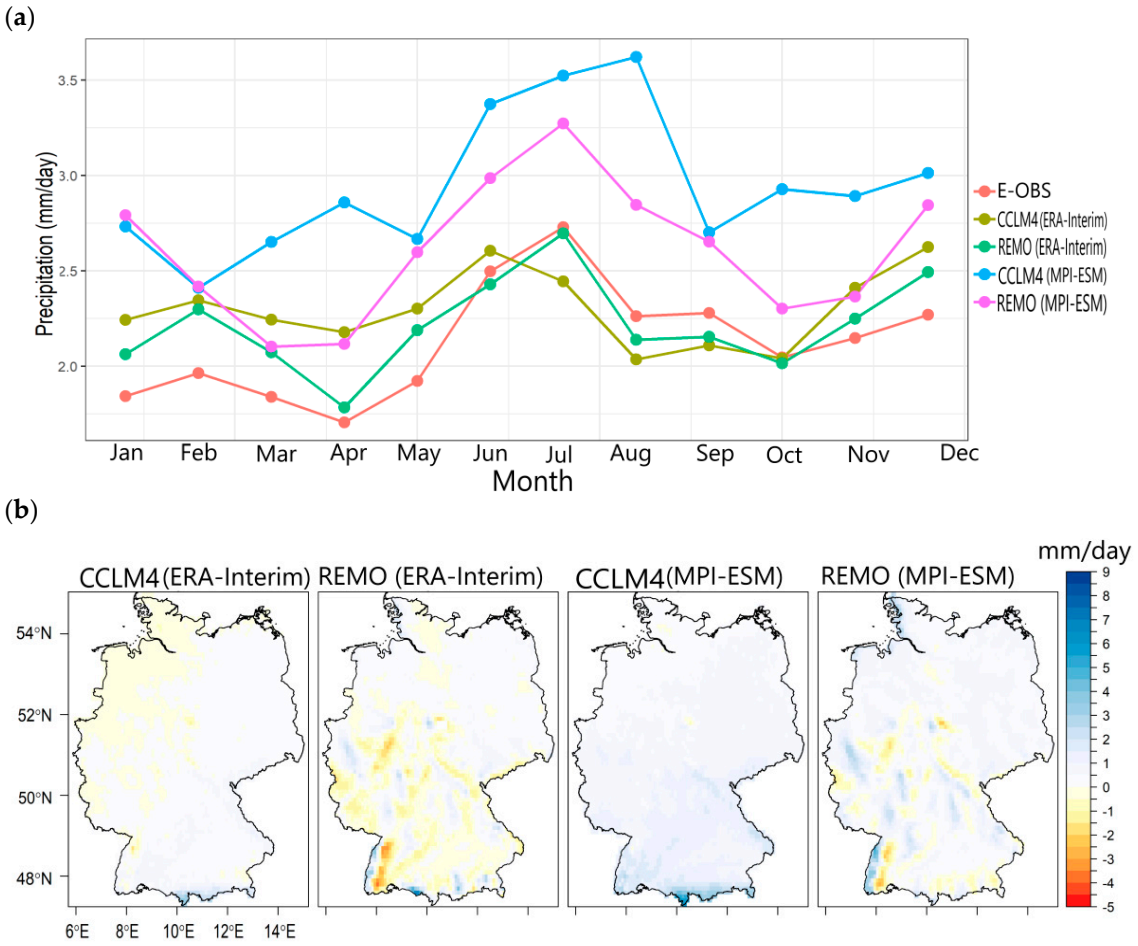

Figure 1. Evaluation of the REMO and CCLM4 RCMs against E-OBS for (**a**) annual cycle and (**b**) spatial mean of precipitation (i.e., RCM minus E-OBS) for the 1989–2005 period.

Spatially, the majority of the biases are located over the southern parts of Germany (Figure 1b). Based on the MAE, Table 1 shows that the precipitation amount is inflated when the RCMs are driven by MPI-ESM. A similar result, that the MPI-ESM induces further wet biases in the RCMs, was reported by [30]. This translates to increasing the wet day biases that become substantially higher when the RCMs are driven by the GCM output (Table 1). Furthermore, in the southwestern part of Germany, there is a dipole pattern of precipitation bias with the REMO model, regardless of the driving data. This suggests that the bias is rather associated with the REMO model. The REMO model shows a dipole-like pattern of precipitation bias in the southwestern parts of Germany. According to [31], this bias can be linked to inadequate orographically induced rainfall over the Rhine valley and Black Forest region.

Table 1. Mean absolute error in the temporal series, spatial series, and annual frequency of wet days from the REMO and CCLM4 RCMs against E-OBS for the 1989–2005 period.

Data Set	MAE (Time) (mm/day)	MAE (Spatial) (mm/day)	Wet Day Bias (day/year)
CCLM4 (ERA-Interim)	1.18	0.26	12
CCLM4 (MPI-ESM)	2.95	0.47	58
REMO (ERA-Interim)	1.40	0.62	18
REMO (MPI-ESM)	2.79	0.81	44

3.2. Relative Performance of the Bias Correction Techniques

Figures 2 and 3 show the performance of the BC during the evaluation period on adjusting seasonal mean precipitation at each grid point in Germany, for the CCLM4 and REMO models, respectively. From Table 2, all BC methods added value in adjusting the biases in the simulated mean precipitation to be closer to observations. The relative performances of the respective BC techniques indicate dependency on the RCM and season analyzed. Most remarkable is that the dipole pattern and local biases in the REMO model were significantly dampened by all the BC methods. Similarly, the localized biases in the southernmost regions under the CCLM4 model were dampened.

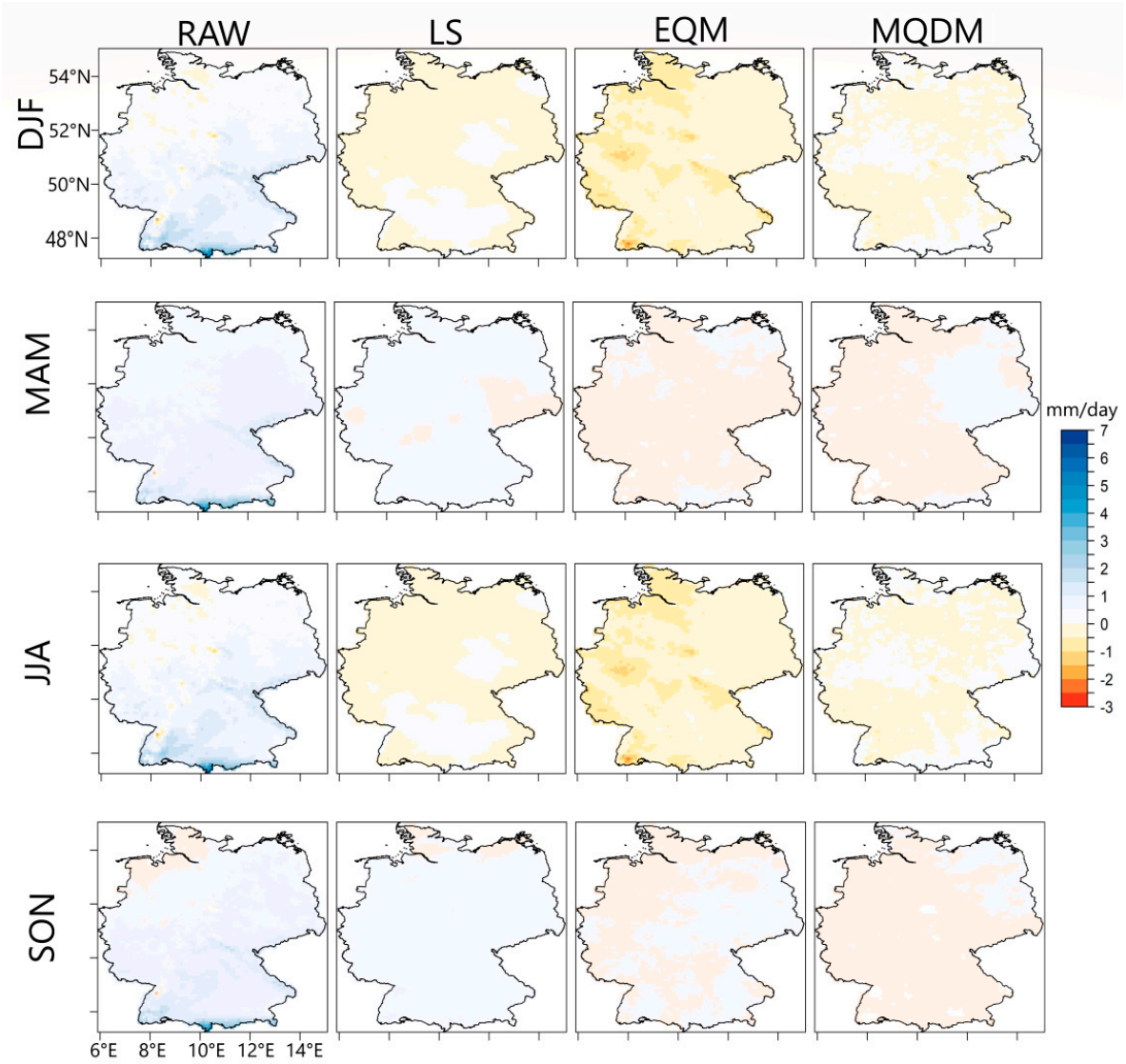

Figure 2. Performance of the bias correction techniques on the spatial mean precipitation as simulated in the CCLM4 RCM, driven by MPI-ESM, during the 1978–2005 evaluation period.

For the CCLM4 model, the EQM increases the biases at some of the grid points, during the DJF and JJA seasons. For the REMO model, the LS method performs best for all seasons in dampening the biases in the simulated mean precipitation at the grid box level. Given that the LS algorithm focuses on scaling the mean precipitation at each grid box to be closer to the observed, this result is not surprising. Nonetheless, the distribution-based methods—i.e., EQM and MQDM—also add value in adjusting the biases in the simulated mean precipitation at most grid boxes.

Figures 4 and 5 show the biases in the spatial variability (i.e., standard deviation) of precipitation at grid points in Germany for the CCLM4 and REMO runs, respectively. As shown by Table 3, the added value in improving the spatial variability of precipitation is slim. The LS method indicates the tendency of worsening the spatial variability of precipitation, depending on the season and RCM. This is more pronounced in the CCLM4 model, where the LS method introduces more biases in the variability of precipitation in large parts of Germany. During DJF, the MQDM method performs well in dampening the biases in the standard deviation and did not worsen the mean bias over Germany, for any of the seasons. Overall, the distribution-based methods perform better in improving the biases in the spatial variability of precipitation over Germany. However, as earlier stated, the performances of the BC techniques in dampening the biases depend on the region, season, and the combination of GCM/RCM. The time (seasonal) dependency of the biases can be partly due to the transient/non-stationarity of the processes associated with precipitation in the study region. For example, seasonal variations in advective flow and atmospheric stability (e.g., [32]). Thus, the associating biases in the simulated precipitation during the distinct seasons can be expected to differ. On the other hand, the spatial dependency of the biases can be associated with the spatial heterogeneity of precipitation in the study region. On the larger scale, the western regions closer to the oceans are wetter, compared to the eastern regions that are farther away from the oceans.

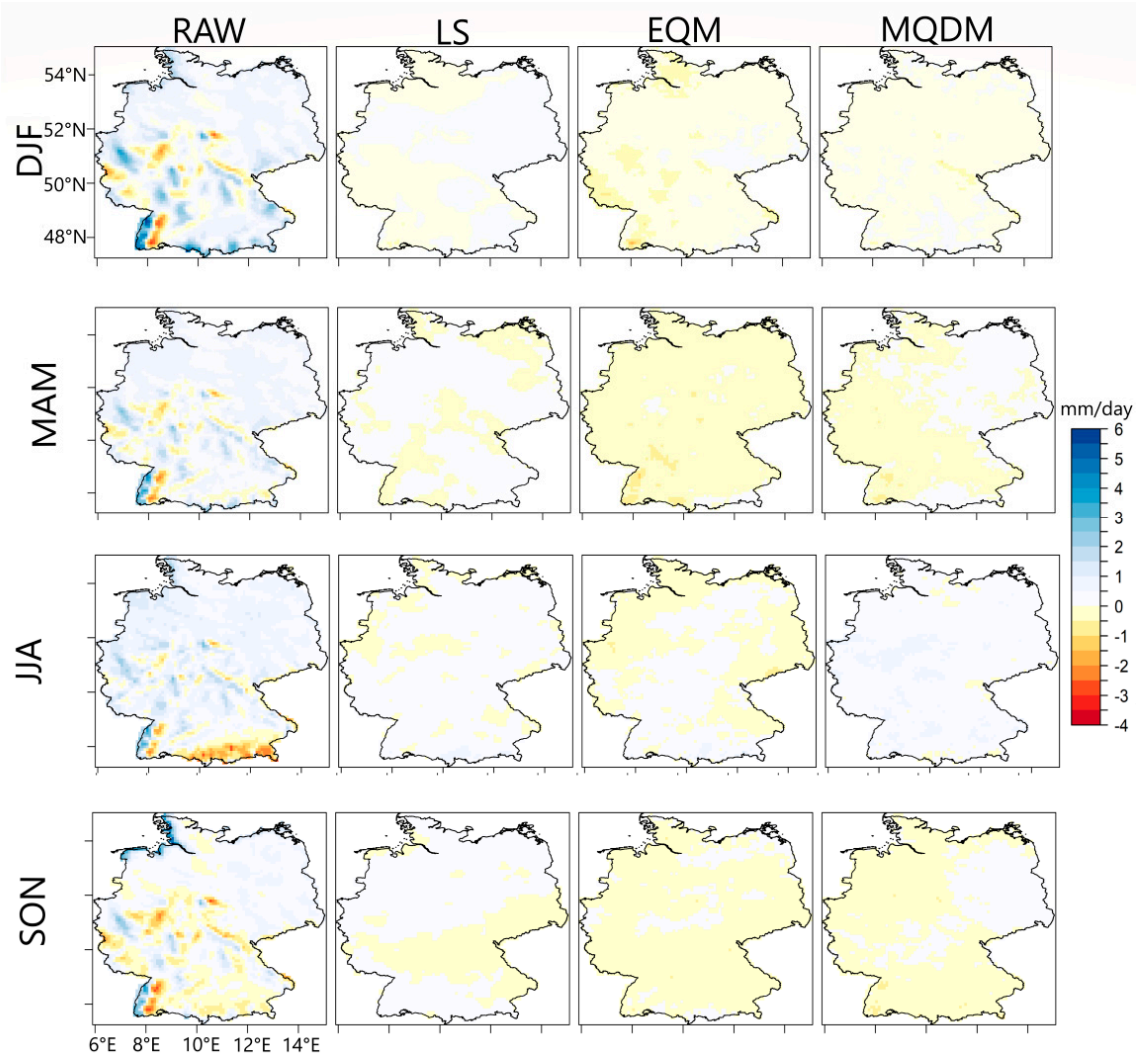

Figure 3. Performance of the bias correction techniques on the spatial mean precipitation as simulated in the REMO RCM, driven by MPI-ESM, during the 1978–2005 evaluation period.

Table 2. Mean absolute error (mm/day) in spatial mean series of the precipitation estimates from the RCMs, driven by MPI-ESM, relative to E-OBS during the 1978–2005 validation period. (*) indicates the best performing BC method, with the lowest error, for a given season.

RAW	LS	EQM	MQDM
	CCLM4		
	DJF		
0.64	0.10 *	0.39	0.10 *
	MAM		
0.63	0.13 *	0.14	0.14
	JJA		
1.03	0.24	0.30	0.17 *
	SON		
0.62	0.19	0.10 *	0.21
	REMO		
	DJF		
0.82	0.08 *	0.27	0.14
	MAM		
0.59	0.08 *	0.20	0.13
	JJA		
0.70	0.11 *	0.15	0.22
	SON		
0.51	0.09 *	0.14	0.15

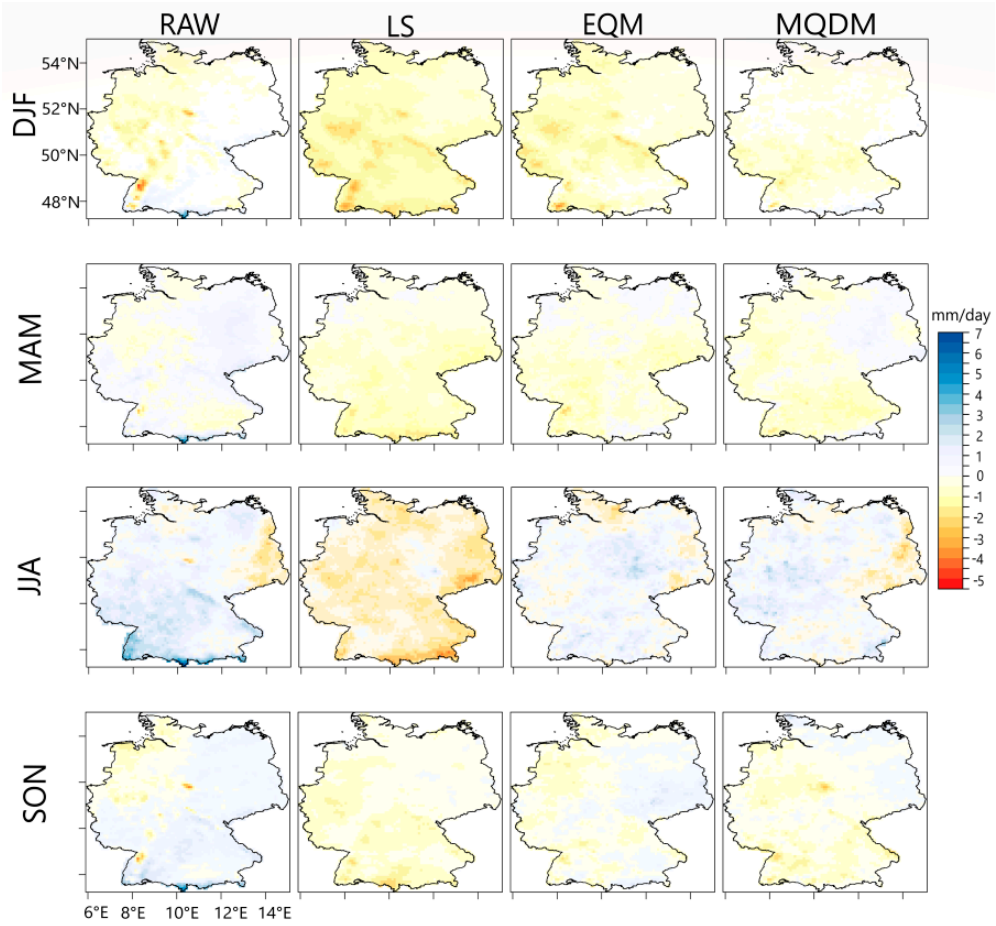

Figure 4. Performance of the bias correction techniques on the spatial variability of precipitation (i.e., standard deviation) as simulated in the CCLM4 RCM, driven by MPI-ESM, during the 1978–2005 evaluation period.

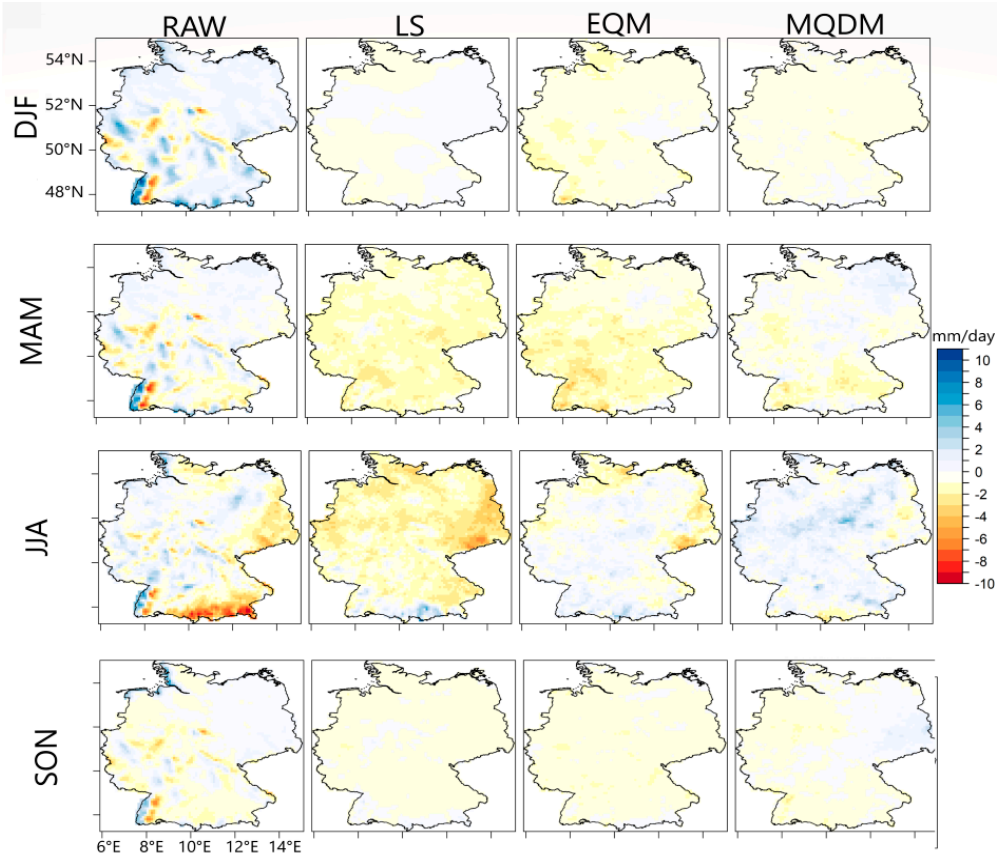

Figure 5. Performance of the bias correction techniques for the spatial variability of precipitation (i.e., standard deviation) as simulated in the REMO RCM, driven by MPI-ESM, during the 1978–2005 evaluation period.

Table 3. Mean absolute error in spatial variability series (i.e., the standard deviation in mm/day) of the precipitation estimates from the RCMs relative to E-OBS during the 1978–2005 validation period. (*) indicates the best performing method and (**) indicates cases where the error is worsened relative to the raw estimates.

Raw	LS	EQM	MQDM
	CCLM4		
	DJF		
0.41	0.87 **	0.55 **	0.25 *
	MAM		
0.43	0.57 **	0.41 *	0.42
	JJA		
0.72	0.73 **	0.42 *	0.44
	SON		
0.48	0.49 **	0.39 *	0.39 *
	REMO		
	DJF		
1.04	0.44	0.45	0.32 *
	MAM		
0.56	0.59 **	0.55	0.33 *
	JJA		
0.74	0.80 **	0.42 *	0.56
	SON		
0.70	0.39 *	0.40	0.41

Next, we evaluate the performance of the BC in terms of the first to four moments of the distribution of daily precipitation time series, averaged over Germany. From the empirical distribution of daily precipitation values before and after the BC, each method adds value in minimizing the wet bias associated with the GCM–RCM model chain (Figure A2). Tables 4 and 5 show the first to fourth moments, as major characteristics of the empirical distributions. Again, the relative performances of the BC techniques depend on the season and RCM. However, the distribution-based BC techniques outperform the LS approach which, in some cases, worsens the third and fourth moments (i.e., skewness and kurtosis). Overall, the MQDM performs best in correcting the biases in the third and fourth moments, whereas EQM increases the biases during SON in the REMO model. The good performance of the LS approach in removing the biases in mean precipitation at the grid point level, especially in REMO (cf. Figure 3), is also illustrated in Table 5 where, for most seasons, it outperforms other methods in adjusting the temporal mean value to the observed one. For the CCLM4 model, the MQDM performs best in improving the first moment. The second-moment quantity, represented by the standard deviation, obviously poses a challenge to the BC methods. In most cases, the Raw RCMs capture the temporal variability better than the corrected precipitation time series. Nonetheless, there are improvements in adjusting the second moment by the MQDM technique. The relatively better performance of the MQDM in improving the higher moments can be linked to the change-preserving attribute of the QDM over the entire distribution, and the incorporation of the spatial dependency of precipitation in the course of the BC.

Table 4. Errors in the first to fourth moments, in mm/day, of the simulated raw and bias-corrected precipitation estimates against observed precipitation values, averaged over Germany, from the CCLM4 model, during the 1978–2005 validation period. Error is calculated as the absolute value of the observed minus simulated statistic. (*), for the RAW values, indicates when the RAW estimate outperforms the corrected values. (*) indicates the best performing BC technique, and (**) indicates third to the fourth moments where the BC technique worsens the statistics.

Statistic	RAW	LS	EQM	MQDM
	DJF			
Mean	0.64	0.08	0.39	0.02 *
SD	0.03 *	0.68	0.56	0.18 *
Skweness	0.42	0.43 **	0.08	0.05 *
Kurtosis	1.77	1.73	0.85	0.44 *
	MAM			
Mean	0.63	0.13	0.12	0.10 *
SD	0.17 *	0.37	0.32	0.25 *
Skweness	0.49	0.36	0.10 *	0.22
Kurtosis	2.27	1.50	0.56 *	1.31
	JJA			
Mean	1.03	0.33	0.23	0.14 *
SD	0.43	0.38	0.02 *	0.06
Skweness	0.43	0.49 **	0.20	0.07 *
Kurtosis	2.17	2.42 **	1.43	0.59 *
	SON			
Mean	0.59	0.18	0.01 *	0.19
SD	0.12 *	0.34	0.23 *	0.37
Skweness	0.48	0.58 **	0.30	0.08 *
Kurtosis	2.45	3.15 **	1.88	0.36 *

To examine the performance of the BC techniques in capturing extreme values of precipitation, we consider return times during boreal summer. First, a GEV distribution is fitted to the annual maximum JJA values of precipitation during the validation period (Figure 6). The results are compared to the observed return times from E-OBS. Second, to assess the sensitivity of the extreme value estimates, we repeat the analysis using the peak-over-threshold approach that is associated with the Gumbel distribution. This approach

might help optimize the calculations given that the sample size can be larger compared to the annual maxima approach. To accommodate more samples, we have used the 90th percentile precipitation value from E-OBS as the threshold. Observed daily precipitation, raw, as well as bias corrected, that exceed this threshold, are used for the return time estimates depicted in Figure 7.

Table 5. Errors in the first to fourth moments, in mm/day, of the simulated raw and bias-corrected precipitation estimates against observed precipitation values, averaged over Germany, from the REMO model, during the 1978–2005 validation period. Error is calculated as the absolute value of the observed minus simulated statistic. (*), for the RAW values, indicates when the RAW estimate outperforms the corrected values. (*) indicates the best performing BC technique, and (**) indicates third to the fourth moments where the BC technique worsens the statistics.

Statistic	RAW	LS	EQM	MQDM
	DJF			
Mean	0.58	0.00 *	0.25	0.11
SD	0.07 *	0.44	0.46	0.43 *
Skweness	0.37	0.36	0.19 *	0.22
Kurtosis	1.52	1.92 **	1.19	0.93 *
	MAM			
Mean	0.50	0.04 *	0.19	0.04 *
SD	0.05 *	0.46	0.32	0.21 *
Skweness	0.23	0.42	0.27	0.08 *
Kurtosis	1.45	1.86 **	1.50 **	1.44 *
	JJA			
Mean	0.51	0.09	0.00 *	0.30
SD	0.14	0.40	0.13	0.00 *
Skweness	0.46	0.26	0.03 *	0.26
Kurtosis	2.06	0.98	0.23 *	0.98
	SON			
Mean	0.24	0.04 **	0.13	0.10
SD	0.06 *	0.33	0.39	0.20 *
Skweness	0.20	0.38 **	0.38 **	0.02 *
Kurtosis	0.57	2.08 **	2.22 **	0.45 *

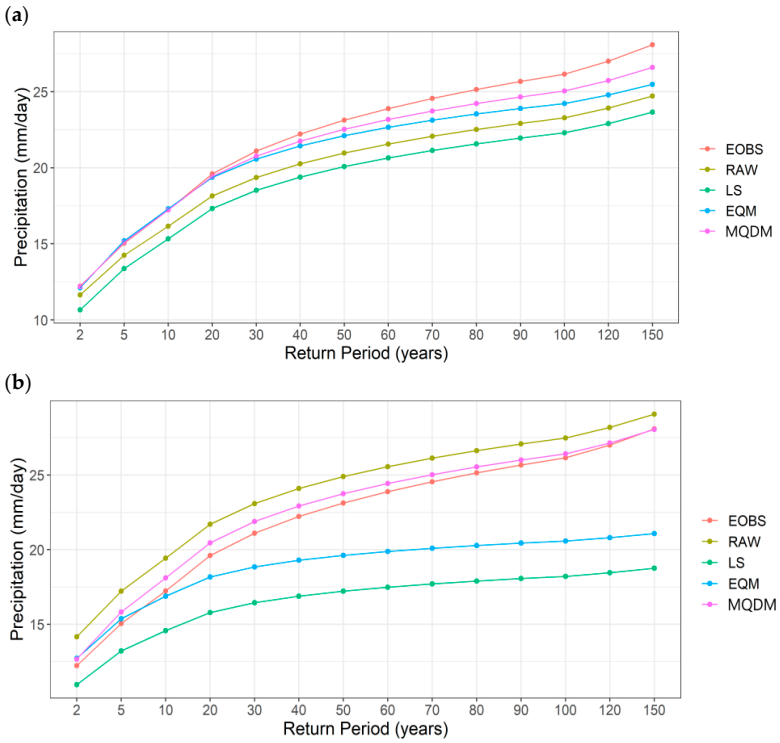

Figure 6. Return level plot of precipitation averaged over Germany from (**a**) REMO and (**b**) CCLM4 before and after bias correction, during JJA in the validation period, using the annual maxima approach and generalized extreme value distribution.

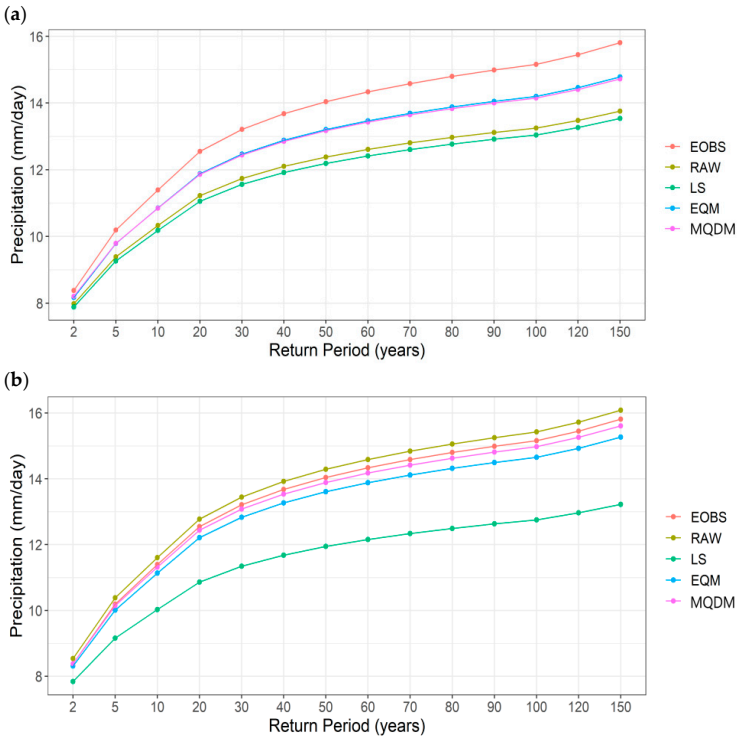

Figure 7. Return level plot of precipitation averaged over Germany from (**a**) REMO and (**b**) CCLM4 before and after bias correction, during JJA in the validation period, using the peak over threshold approach and Gumbel distribution.

Figure 6 shows that based on the GEV distribution, the observed return times are best represented by the MQDM approach. Concerning MAE, MQDM outperforms other

methods by a large margin in both RCMs. For the peak-over-threshold approach, the results are a bit different compared to the annual maxima approach. Ref. [33] reported that in terms of extreme events, the peak-over-threshold approach can be relatively more robust. This is also confirmed in our results based on the Gumbel model fit. Figure 7 shows that similar to the annual maxima approach, the MQDM output is closest to observations in the CCLM4 model, whereas in REMO, the EQM outperforms the MQDM with a slim margin (based on the MAE). In all cases, the LS approach worsens the estimate of return times by the RCMs. Overall, the MQDM outperforms the other methods in adjusting summer extreme precipitation characteristics across Germany to the observed values. [14] reported also that, compared to the EQM, the QDM, which is implemented in the MQDM algorithm, performs better in correcting precipitation extremes. Since the change signal is incorporated in the MQDM, it is reasonable that it performs well in capturing precipitation extremes during JJA in Germany.

4. Conclusions and Outlook

The relative performance of three BC techniques in adjusting the biases in simulated precipitation from the RCMs, CCLM4 and REMO (driven by MPI-ESM-LR) over Germany is examined in this work. The BC techniques being considered here are the LS method that adjusts the biases in the mean, and two distribution-based methods—i.e., the EQM and MQDM. The MQDM is a multivariate BC technique, implemented with the QDM that preserves climate change signals in the quantiles. Here we used grids that covary as variables, in an effort to incorporate the spatial dependency of the precipitation, in the course of the BC. Our results show that the performance of the methods depends on (i) the season analyzed; (ii) the choice of the GCM/RCM model chain; (iii) the region; (iv) and the statistical metrics considered. The LS method performs well in improving the first moment but shows a tendency in worsening the higher moments and the representation of precipitation extremes. Overall, the MQDM outperforms the EQM in adjusting the higher moments and the extremes in precipitation, during summer. Hence, we conclude that the MQDM has the potential to adjust biases in simulated precipitation over Germany and might be applied preferably when it comes to providing reliable distributions of precipitation, e.g., for impact modeling and adaptation studies.

The present study is restricted to only two RCMs out of the EURO-CORDEX ensemble because the described work has been motivated by the framework of the German RegIKLim project. In this project, very high-resolution climate change projections will be provided for seven model regions across Germany where various attempts of impact modeling are carried out and adaptation strategies to climate change will be elaborated. The project is based on new RCM versions from the German modeler communities, i.e., REMO, CCLM and ICON. From a more general climatological perspective, it would also be of interest to assess to what extent these results might be corroborated by different GCM–RCM combinations that are available for central Europe—a matter of ongoing research.

This publication was supported by the Open Access Publication Fund of the University of Wuerzburg. VAT DE 134187690.

Author Contributions: Conceptualization, C.C.I., H.P., E.X., D.S. and M.A.; methodology, C.C.I., H.P., E.X., D.S. and M.A.; software, C.C.I., D.S. and M.A.; validation, C.C.I., H.P., E.X., D.S. and M.A.; formal analysis, C.C.I., H.P., E.X., D.S. and M.A.; investigation, C.C.I., H.P., E.X., D.S. and M.A.; resources, H.P. and E.X.; data curation, C.C.I., D.S. and M.A.; writing—original draft preparation, C.C.I.; writing—review and editing, C.C.I., H.P., E.X., D.S. and M.A.; visualization, C.C.I., H.P., E.X., D.S. and M.A.; supervision, H.P. and E.X.; project administration, H.P. and E.X.; funding acquisition, H.P. and E.X. All authors have read and agreed to the published version of the manuscript.

Funding: The study has been funded by the RegIKlim project of the German Ministry of Education and Research under grants 01LR2002D and 01LR2002F.

Institutional Review Board Statement: Not applicable.

Informed Consent Statement: Not applicable.

Data Availability Statement: The CMIP5 models are available at https://esgf-data.dkrz.de/projects/esgf-dkrz/ (accessed on 20 November 2021). The E-OBS data is available at https://www.ecad.eu (accessed on 20 November 2021).

Conflicts of Interest: The authors declare no conflict of interest.

Appendix A

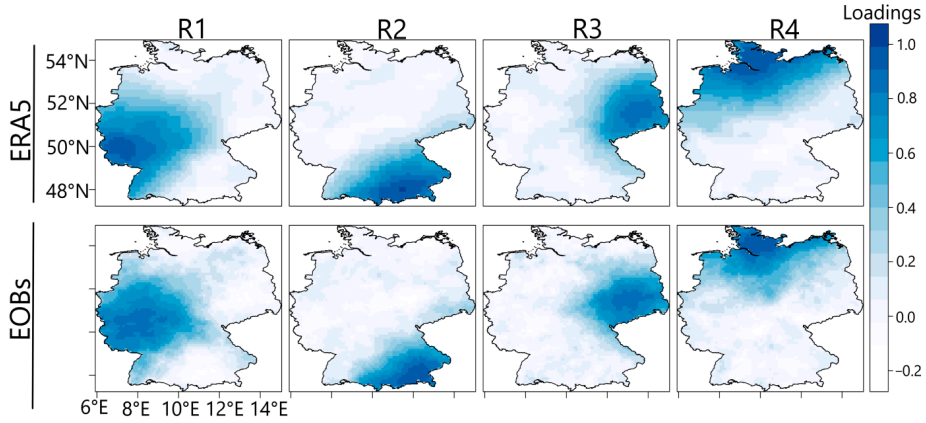

Figure A1. Leading four homogeneous regions of rainfall anomalies in Germany from E-OBS and ERA5. The regions are obtained using the rotated S-mode PCA. Only rotated PCs that match with the correlation structure with a congruence match of at least 0.9 are kept and designated to represent physically interpretable patterns. The patterns are also reproduced when the analysis period is changed (not shown).

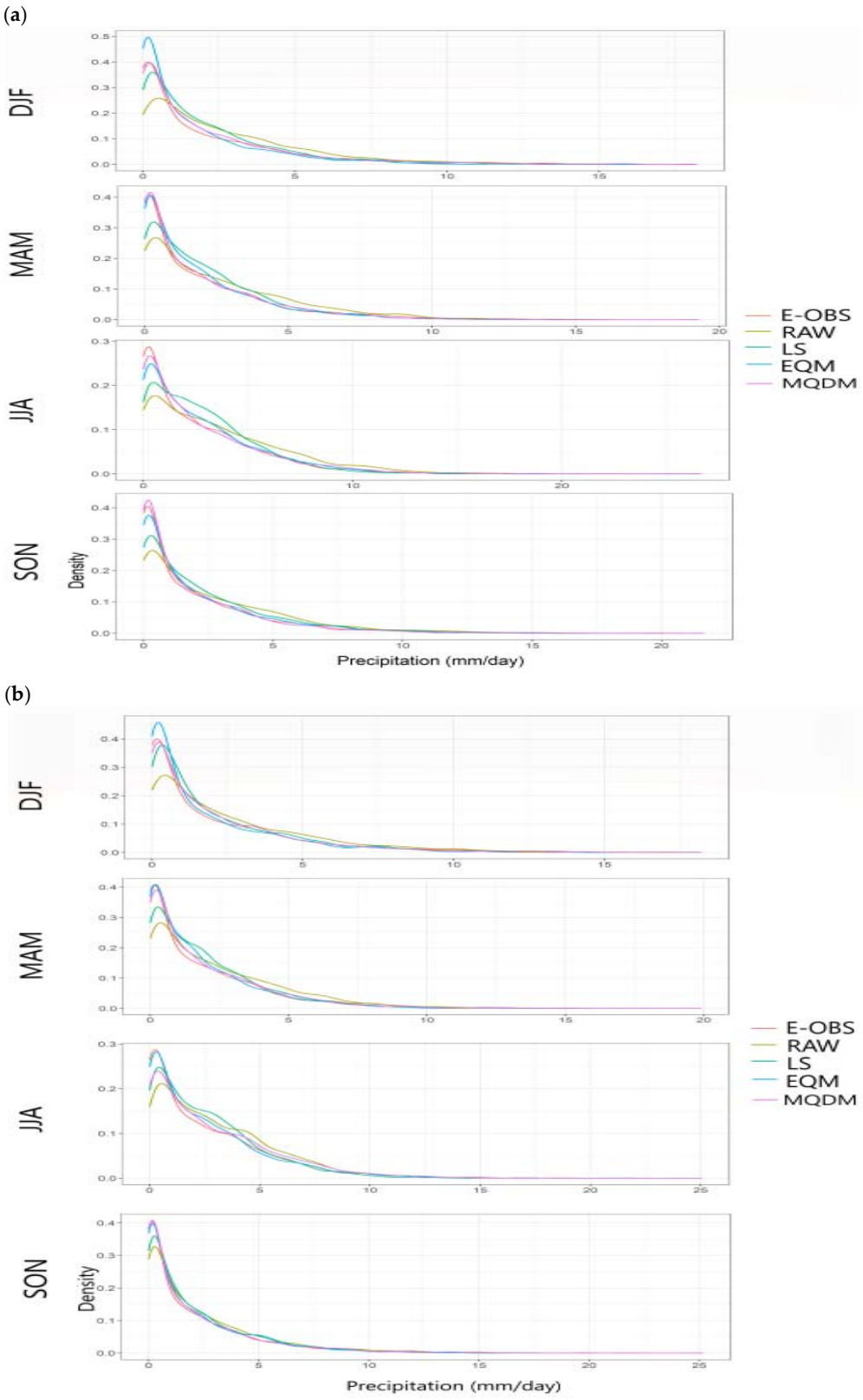

Figure A2. Distribution of the simulated raw, bias-corrected, and observed precipitation values, averaged over Germany, from REMO (**a**) and CCLM4, (**b**) RCMs, for the 1978–2005 validation period.

References

1. Kotlarski, S.; Keuler, K.; Christensen, O.B.; Colette, A.; Déqué, M.; Gobiet, A.; Goergen, K.; Jacob, D.; Lüthi, D.; van Meijgaard, E.; et al. Regional climate modeling on European scales: A joint standard evaluation of the EURO-CORDEX RCM ensemble. *Geosci. Model Dev.* **2014**, *7*, 1297–1333. [CrossRef]
2. Paeth, H.; Born, K.; Podzun, R.; Jacob, D. Regional dynamical downscaling over West Africa: Model evaluation and comparison of wet and dry years. *Meteorol. Z.* **2005**, *14*, 349–367. [CrossRef]
3. Paeth, H.; Born, K.; Girmes, R.; Podzun, R.; Jacob, D. Regional Climate Change in Tropical and Northern Africa due to Greenhouse Forcing and Land Use Changes. *J. Clim.* **2009**, *22*, 114–132. [CrossRef]
4. Fowler, H.J.; Blenkinsop, S.; Tebaldi, C. Linking climate change modelling to impacts studies: Recent advances in downscaling techniques for hydrological modelling. *Int. J. Clim.* **2007**, *27*, 1547–1578. [CrossRef]
5. Maraun, D.; Wetterhall, F.; Ireson, A.M.; Chandler, R.E.; Kendon, E.J.; Widmann, M.; Brienen, S.; Rust, H.W.; Sauter, T.; Themeßl, M.; et al. Precipitation downscaling under climate change: Recent developments to bridge the gap between dynamical models and the end user. *Rev. Geophys.* **2010**, *48*. [CrossRef]
6. Eden, J.M.; Widmann, M.; Grawe, D.; Rast, S. Skill, Correction, and Downscaling of GCM-Simulated Precipitation. *J. Clim.* **2012**, *25*, 3970–3984. [CrossRef]
7. Maraun, D.; Widmann, M. The representation of location by regional climate models in complex terrain. *Hydrol. Earth Syst. Sci. Discuss.* **2015**, *12*, 3011–3028. [CrossRef]
8. Gutiérrez, J.M.; Maraun, D.; Widmann, M.; Huth, R.; Hertig, E.; Benestad, R.; Roessler, O.; Wibig, J.; Wilcke, R.; Kotlarski, S.; et al. An intercomparison of a large ensemble of statistical downscaling methods over Europe: Results from the VALUE perfect predictor cross-validation experiment. *Int. J. Clim.* **2018**, *39*, 3750–3785. [CrossRef]
9. Paeth, H.; Girmes, R.; Menz, G.; Hense, A. Improving Seasonal Forecasting in the Low Latitudes. *Mon. Weather Rev.* **2006**, *134*, 1859–1879. [CrossRef]
10. Paeth, H. Postprocessing of simulated precipitation for impact research in West Africa. Part I: Model output statistics for monthly data. *Clim. Dyn.* **2011**, *36*, 1321–1336. [CrossRef]
11. Paeth, H.; Diederich, M. Postprocessing of simulated precipitation for impact research in West Africa. Part II: A weather generator for daily data. *Clim. Dyn.* **2011**, *36*, 1337–1348. [CrossRef]
12. Chen, J.; Brissette, F.P.; Chaumont, D.; Braun, M. Finding appropriate bias correction methods in downscaling precipitation for hydrologic impact studies over North America. *Water Resour. Res.* **2013**, *49*, 4187–4205. [CrossRef]
13. Dosio, A.; Paruolo, P.; Rojas, R. Bias correction of the ENSEMBLES high resolution climate change projections for use by impact models: Analysis of the climate change signal. *J. Geophys. Res. Earth Surf.* **2012**, *117*. [CrossRef]
14. Cannon, A.J.; Sobie, S.R.; Murdock, T.Q. Bias Correction of GCM Precipitation by Quantile Mapping: How Well Do Methods Preserve Changes in Quantiles and Extremes? *J. Clim.* **2015**, *28*, 6938–6959. [CrossRef]
15. Maurer, E.P.; Pierce, D.W. Bias correction can modify climate model simulated precipitation changes without adverse effect on the ensemble mean. *Hydrol. Earth Syst. Sci.* **2014**, *18*, 915–925. [CrossRef]
16. Wood, A.; Leung, L.R.; Sridhar, V.; Lettenmaier, D.P. Hydrologic Implications of Dynamical and Statistical Approaches to Downscaling Climate Model Outputs. *Clim. Chang.* **2004**, *62*, 189–216. [CrossRef]
17. Bürger, G.; Sobie, S.R.; Cannon, A.; Werner, A.T.; Murdock, T.Q. Downscaling Extremes: An Intercomparison of Multiple Methods for Future Climate. *J. Clim.* **2013**, *26*, 3429–3449. [CrossRef]
18. Willkofer, F.; Schmid, F.-J.; Komischke, H.; Korck, J.; Braun, M.; Ludwig, R. The impact of bias correcting regional climate model results on hydrological indicators for Bavarian catchments. *J. Hydrol. Reg. Stud.* **2018**, *19*, 25–41. [CrossRef]
19. Lenderink, G.; van Ulden, A.; Hurk, B.V.D.; Keller, F. A study on combining global and regional climate model results for generating climate scenarios of temperature and precipitation for the Netherlands. *Clim. Dyn.* **2007**, *29*, 157–176. [CrossRef]
20. Berg, P.; Feldmann, H.; Panitz, H.-J. Bias correction of high resolution regional climate model data. *J. Hydrol.* **2012**, *448–449*, 80–92. [CrossRef]
21. Rocheta, E.; Evans, J.; Sharma, A. Assessing atmospheric bias correction for dynamical consistency using potential vorticity. *Environ. Res. Lett.* **2014**, *9*, 124010. [CrossRef]
22. Nelsen, R.B. *An Introduction to Copulas*, 2nd ed.; Springer: Berlin, Germany, 2006. [CrossRef]
23. Mao, G.; Vogl, S.; Laux, P.; Wagner, S.; Kunstmann, H. Stochastic bias correction of dynamically downscaled precipitation fields for Germany through Copula-based integration of gridded observation data. *Hydrol. Earth Syst. Sci.* **2015**, *19*, 1787–1806. [CrossRef]
24. Maity, R.; Suman, M.; Laux, P.; Kunstmann, H. Bias Correction of Zero-Inflated RCM Precipitation Fields: A Copula-Based Scheme for Both Mean and Extreme Conditions. *J. Hydrometeorol.* **2019**, *20*, 595–611. [CrossRef]
25. Cannon, A.J. Multivariate quantile mapping bias correction: An N-dimensional probability density function transform for climate model simulations of multiple variables. *Clim. Dyn.* **2017**, *50*, 31–49. [CrossRef]
26. Jacob, D.; Petersen, J.; Eggert, B.; Alias, A.; Christensen, O.B.; Bouwer, L.M.; Braun, A.; Colette, A.; Déqué, M.; Georgievski, G.; et al. EURO-CORDEX: New high-resolution climate change projections for European impact research. *Reg. Environ. Chang.* **2014**, *14*, 563–578. [CrossRef]
27. Popke, D.; Stevens, B.; Voigt, A. Climate and climate change in a radiative-convective equilibrium version of ECHAM6. *J. Adv. Modeling Earth Syst.* **2013**, *5*, 1–14. [CrossRef]

28. Cornes, R.C.; Van Der Schrier, G.; van den Besselaar, E.J.M.; Jones, P.D. An Ensemble Version of the E-OBS Temperature and Precipitation Data Sets. *J. Geophys. Res. Atmos.* **2018**, *123*, 9391–9409. [CrossRef]
29. Jones, P.W. First-and second-order conservative remapping schemes for grids in spherical coordinates. *Mon. Weather Rev.* **1999**, *127*, 2204–2210. [CrossRef]
30. Teichmann, C.; Eggert, B.; Elizalde, A.; Haensler, A.; Jacob, D.; Kumar, P.; Moseley, C.; Pfeifer, S.; Rechid, D.; Remedio, A.R.; et al. How Does a Regional Climate Model Modify the Projected Climate Change Signal of the Driving GCM: A Study over Different CORDEX Regions Using REMO. *Atmosphere* **2013**, *4*, 214–236. [CrossRef]
31. Feldmann, H.; Früh, B.; Schädler, G.; Panitz, H.-J.; Keuler, K.; Jacob, D.; Lorenz, P. Evaluation of the precipitation for South-western Germany from high resolution simulations with regional climate models. *Meteorol. Z.* **2008**, *17*, 455–465. [CrossRef]
32. Ibebuchi, C. Patterns of atmospheric circulation in Western Europe linked to heavy rainfall in Germany: Preliminary analysis into the 2021 heavy rainfall episode. *Theor. Appl. Climatol.* **2022**. [CrossRef]
33. Fischer, S.; Schumann, A. Comparison between Classical Annual Maxima and Peak over Threshold Approach Concerning Robustness. 2014. Available online: https://eldorado.tu-dortmund.de/handle/2003/33522 (accessed on 20 December 2021).